DOI: 10.1002/ejoc.200900471

# Triphenylamine-Based Pyridine *N*-Oxide and Pyridinium Salts for Size-Selective Recognition of Dicarboxylates

**Kumaresh Ghosh,*[a] Goutam Masanta,[a] and Asoke P. Chattopadhyay[a]**

**Keywords:** Receptors / Anions / Anion recognition / Fluorimetric detection

Triphenylamine-based receptors **1**–**3** have been designed and synthesized for the recognition of dicarboxylates. The correct dispositions of the binding groups in both **1** and **2** under 4,4′-dicarbonyltriphenylamine spacer enable them to bind aliphatic dicarboxylates of different chain lengths with moderate binding constant values. In the binding event, triphenylamine-based pyridinium salt **2** is found to be more effective than triphenylamine-based pyridine *N*-oxide **1** and shows selectivity for long-chain pimelate. Binding takes place at charged sites with concomitant PET-based (photoinduced electron transfer) quenching of emission of triphenylamine motif. The binding was monitored in DMSO using $^1$H NMR, UV/Vis and fluorescence spectroscopic methods. Efficiency of pyridinium binding site over the others in the present study has been rationalised by invoking theoretical results.


## Introduction

The design and synthesis of fluorogenic chemosensors for selective recognition of biologically important anions is of current interest in the field of supramolecular chemistry.[1] Dicarboxylates are among the most attractive targets for anion recognition and sensing because of their considerable role in biological systems.[2] Various reports on sensing of dicarboxylates involving different binding motifs such as polyprotonated azacrown,[3] guanidinium,[4] polyammonium,[5] imidazolium,[6] urea/thiourea[2b,7] etc., appended to suitable chromophores or fluorophores as signaling probes, have been reported. However, the use of the pyridinium motif in the construction of a fluorescent receptor for dicarboxylates is less explored. Recently, Steed and co-workers reported ureidopyridyl-based tripodal receptors for selective recognition of chloride ions.[8] The use of a C–H···X hydrogen bond as offered by the pyridinium motif in complexing guest species is the key feature of pyridinium-based receptors. The importance of C–H···X bonds over the strong N–H···X and O–H···X (X = N, O) hydrogen bonds is of current interest because C–H···X hydrogen bonds play an important role in the stabilization of nucleobase quartet,[9] $^t$RNA structure,[10] and many crystal structures.[11] Within the scope of our investigations on the development of receptors for selective recognition of dicarboxylates, we herein report our results on the synthesis and dicarboxylate anion binding behavior of new triphenylamine-labelled bis(pyridine *N*-oxide) and bis(pyridinium salt) receptors **1** and **2**, respectively, where C–H···O hydrogen bonds have been taken into account to stabilize the complexes.

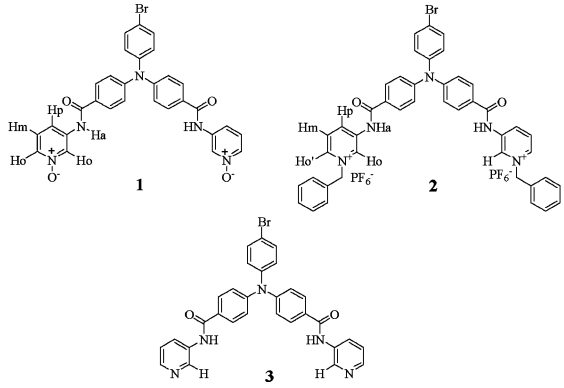


Previously, we have reported for the first time on the use of triphenylamine as a fluorescent probe in the construction of receptors for dicarboxylic acids.[12] For further exploration we have introduced this motif as a fluorescent probe in devising molecular receptors for selective binding of dicarboxylate. So far there are no triphenylamine-based synthetic receptors known in the literature for molecular recognition studies on dicarboxylates. In order to get the new receptors **1** and **2**, we have installed amido pyridine *N*-oxide and pyridinium motifs onto the triphenylamine motif as binding sites. The complexation abilities of such motifs were compared with the pyridinecarboxamide-based receptor **3**.

[a] Department of Chemistry, University of Kalyani, Kalyani, Nadia 741235, India
Fax: +91-3325828282
E-mail: ghosh_k2003@yahoo.co.in
Supporting information for this article is available on the WWW under http://dx.doi.org/10.1002/ejoc.200900471.

  

## Results and Discussion

The syntheses of **1**, **2** and **3** were accomplished according to Scheme 1. Triphenylamine was formylated by using $POCl_3$/DMF to yield mono-, di- and tri-formylated products.[13] The desired 4,4′-diformyltriphenylamine **4a** was isolated in 57% yield, which on bromination followed by oxidation of the aldehydic groups gave the compound **6**. Subsequent reaction of **6** with oxalyl chloride in dry $CH_2Cl_2$ yielded the diacid chloride **7** which on coupling with 3-aminopyridine gave the receptor **3** in 68% yield as light yellow powder. On oxidation with *m*-CPBA, receptor **3** gave **1** in 45% yield as a white solid. On the other hand, receptor **2** was obtained as a light green solid in 88% yield by the reaction of **3** with benzyl bromide followed by anion exchange with $NH_4PF_6$. All these compounds were characterized by usual spectroscopic techniques.

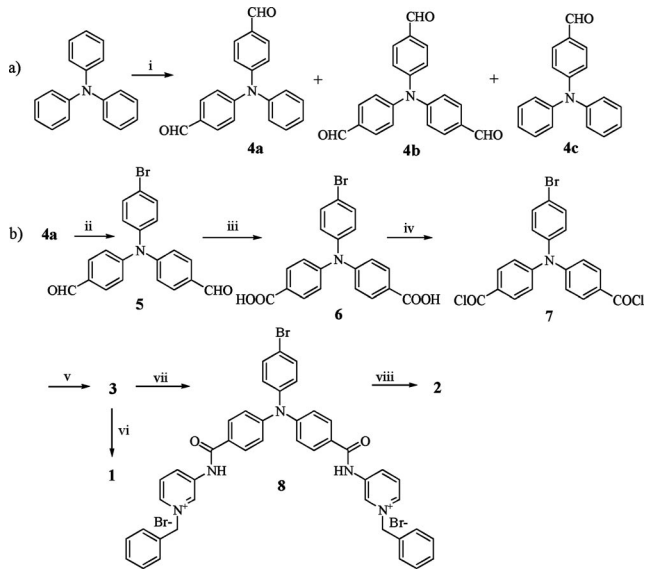

Scheme 1. Reagents and conditions: **a**: (i) $POCl_3$, DMF, reflux, 8 h; **b**: (ii) NBS, dry $CHCl_3$, reflux, 8 h; (iii) $KMnO_4$, acetone/water, reflux, 8 h; (iv) oxalyl chloride, DMF, dry $CH_2Cl_2$, room temp., 9 h; (v) 3-aminopyridine, $Et_3N$, dry THF, room temp., 18 h; (vi) *m*-CPBA, dry $CHCl_3$, reflux, 9 h; (vii) benzyl bromide, dry $CH_3CN$, reflux, 22 h; (viii) $NH_4PF_6$, methanol.

The acyclic receptors **1**, **2** and **3** can exhibit different conformations depending on the orientation of the binding sites. The required conformations were energy optimized in gas phase to realize the cavity dimensions as well as orientation of the binding groups.[14] Figure 1 (a–**c**) represents the energy-optimized geometries of **1**, **2** and **3**, respectively. Also, the optimization of receptor **2**, for example, was done with different dicarboxylates to realize their best fitting into cavity of receptor **2** (see Supporting Information). Among the dicarboxylates, long-chain pimelate formed a stable complex with **2** in the gas phase.

The complexation abilities of receptors **1**–**3** towards aliphatic dicarboxylates of different chain lengths were investigated by $^1$H NMR in [$D_6$]DMSO, fluorescence and UV/Vis studies in DMSO.

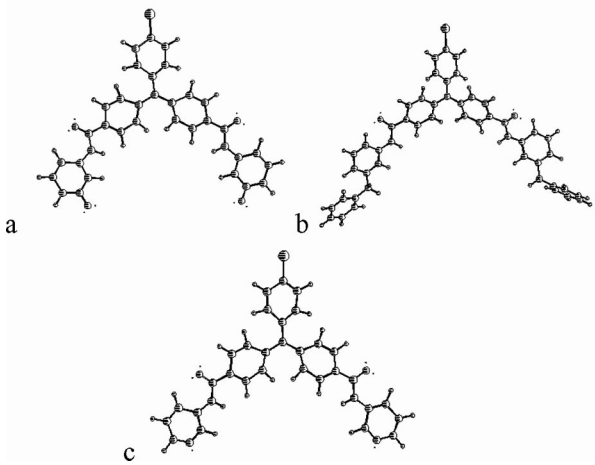

Figure 1. **a**: Energy-optimized geometry of **1**; $E_{min}$ = 158.588 kcal mol$^{-1}$; $d_{NHa–NHa}$ = 8.91 Å, $d_{Ho–Ho}$ = 9.28 Å. **b**: Energy-optimized geometry of **2**; $E_{min}$ = 135.269 kcal mol$^{-1}$; $d_{NHa–NHa}$ = 9.45 Å, $d_{Ho–H0}$ = 11.341 Å. **c**: Energy-optimized geometry of **192**; $E_{min}$ = 177.35 kcal mol$^{-1}$; $d_{NHa–NHa}$ = 9.21 Å $d_{Ho–Ho}$ = 10.64 Å.

### $^1$H NMR Study

To investigate the hydrogen bonding interactions, we initially studied the $^1$H NMR spectrum of **1** in [$D_6$]DMSO in the absence and presence of aliphatic dicarboxylates of different chain lengths. Addition of aliphatic dicarboxylates (malonate, succinate, glutarate, adipate, pimelate, suberate, all of them as tetrabutylammonium salts) to a solution of receptor **1** in [$D_6$]DMSO (as [H]/[G] = 1:1 composition) resulted in large downfield shifts of $H^o$, $H^p$ and $NH_a$ protons owing to the formation of a receptor **1**–dicarboxylate complex. It is worthwhile to note that the signals for the $H^o$, $H^p$ and $NH_a$ protons in **1** significantly moved downfield, while signals for $H^{o'}$ and $H^m$ protons underwent slight upfield-shift ($\Delta\delta \approx 0.07$ ppm). The extent of change in chemical shift of the protons ($H^o$, $H^p$ and $H_a$) was different for different dicarboxylates. Table 1 shows the change in chemical shift of different protons of the pyridinecarboxamide motif in **1** when equivalent amounts of different aliphatic dicarboxylates were separately added to the [$D_6$]DMSO solution of **1**. It is evident from Table 1 that the change in chemical shift is significant in case of long-chain dicarboxylates such as pimelate and suberate. We suggest that such downfield chemical shifts of both $H^o$ and $H^p$, are due to the formation of a weak C–H···O hydrogen bond with the carboxylate anion. Simultaneous involvement of amide proton ($H_a$), ring protons $H^o$ and $H^p$ of pyridine *N*-oxide motif in **1** stabilizes the complex between **1** and carboxylate anion. Figure 2 shows the partial $^1$H NMR spectra of the 1:1 complexes of **1** with pimelate and suberate. In relation to this, two binding modes are possible; this assumption is supported by the significant $^1$H-NMR downfield shifts for the $H^o$ and $H^p$ protons (see Table 1).

Forms **A** and **B** in Figure 3 illustrate the formation of 1:1 host-to-guest complex where possibilities of involvement of both $H^o$ and $H^p$ in hydrogen bonding have been shown and both the forms may remain in equilibrium in solution. In-

  

Table 1. Change in chemical shift values of the participating protons of receptor **1** in 1:1 complexes with various anions.[a]

| Guest | $\Delta\delta$ for $NH_a$ [ppm] | $\Delta\delta$ for $H^o$ [ppm] | $\Delta\delta$ for $H^p$ [ppm] | $\Delta\delta$ for $H^{o'}$ [ppm] | $\Delta\delta$ for $H^m$ [ppm] |
|---|---|---|---|---|---|
| Malonate | 0.02 + | 0.02 – | 0.01 – | 0.13 – | 0.1 – |
| Succinate | 0.03 + | 0.01 + | 0.02 + | 0 | 0 |
| Glutarate | 1.10 + | 0.08 + | 0.09 + | 0.09 – | 0.07 – |
| Adipate | 1.42 + | 0.12 + | 0.12 + | 0.06 – | 0.05 – |
| Pimelate | 1.70 + | 0.15 + | 0.22 + | 0.06 – | 0.06 – |
| Suberate | 1.40 + | 0.11 + | 0.14 + | 0.07 – | 0.06 – |

[a] '+' indicates downfield chemical shift; '–' indicates upfield chemical shift.

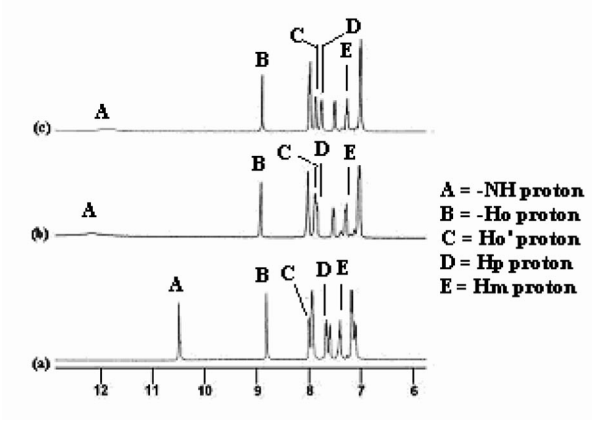


Figure 2. Partial $^1H$ NMR spectra of **1** ($c = 2.64 \times 10^{-3}$ M) with pimelate in [$D_6$]DMSO, (a) **1** only and (b) 1:1 complex with pimelate (c) 1:1 complex with suberate.

volvement of the $H^o$ proton of one pyridine *N*-oxide and $H^p$ proton of another pyridine *N*-oxide motif in the complexation of dicarboxylate, although difficult to predict on the NMR time scale, cannot be ignored (form **C** in Figure 3). Dicarboxylates which are unable to bridge the binding sites may form 1:2 host-to-guest complex (form **D** in Figure 3).

Likewise, the change in chemical shift values of $H^o$, $H^p$ and $NH_a$ protons of **2** was noted in the presence of the same dicarboxylates as taken for **1**. It was found that changes of chemical shift were much higher than that of **1** (Table 2). This is attributed to the greater acidity of $H^o$ and $H^p$ protons of **2** as compared to that of receptor **1**. The amide signal in each case was difficult to detect accurately due to significant broadening upon complexation.

It is also evident from Table 2 that greater changes in chemical shift are observed for pimelate and suberate. Like **1** the possible modes of binding of **2** with the dicarboxylates are suggested in Figure 4.

$^1H$ NMR spectra of **2** and its 1:1 complexes with pimelate and suberate are displayed in Figure 5. On the contrary, receptor **3** did not show any complexation induced significant change in chemical shift of both $H^o$ and $H^p$ protons as that of **1** and **2**. Only the amide protons exhibited measurable downfield chemical shift upon complexation. For example, changes in chemical shift values for $H^o$, $H^p$ and amide NH in **3** are 0.14, 0.08 and 1.13 ppm, respectively,

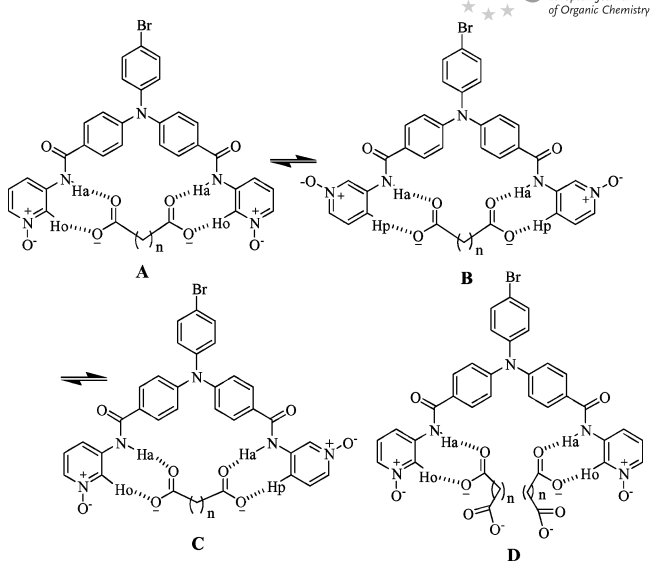


Figure 3. Possible modes of binding of **1** with dicarboxylates in solution.

Table 2. Change in chemical shift values of the participating protons of receptor **2** in 1:1 complexes with various anions.[a]

| Guest | $\Delta\delta$ for $NH_a$ [ppm] | $\Delta\delta$ for $H^o$ [ppm] | $\Delta\delta$ for $H^p$ [ppm] | $\Delta\delta$ for $H^{o'}$ [ppm] | $\Delta\delta$ for $H^m$ [ppm] |
|---|---|---|---|---|---|
| Malonate | a | 0.10 + | 0.14 + | 0.03 – | 0.03 – |
| Succinate | a | 0.09 + | 0.11 + | 0.03 – | 0.03 – |
| Glutarate | a | 0.21 + | 0.11 + | 0.09 – | 0.08 – |
| Adipate | a | 0.21 + | 0.24 + | 0.09 – | 0.08 – |
| Pimelate | a | 0.22 + | 0.25 + | 0.13 – | 0.11 – |
| Suberate | a | 0.22 + | 0.25 + | 0.10 – | 0.09 – |

[a] '+' indicates downfield chemical shift; '–' indicates upfield chemical shift. 'a' indicates broadening of the amide signal for which detection was difficult.

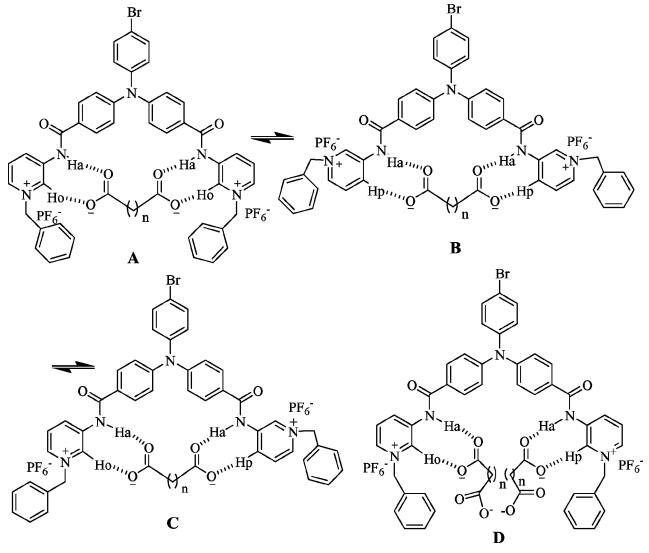


Figure 4. Possible modes of binding of **2** with dicarboxylates in solution.

  

upon complexation of pimelate (1:1 stoichiometry). Negligible change in chemical shift of $H^o$ as well as $H^p$ protons of **3** indicated that the receptor **3** is less efficient in forming more number of hydrogen bonds with dicarboxylates like **1** and **2** as suggested in Figures 3 and 4. After establishing the binding sites that are interacting with dicarboxylates we performed fluorescence and UV studies to determine the binding potencies as well as selectivities.

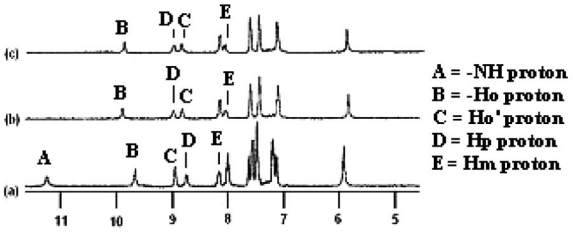


Figure 5. Partial $^1$H NMR spectra of **2** ($c = 2.62 \times 10^{-3}$ M) with pimelate and suberate in [$D_6$]DMSO, (a) **2** only and (b) 1:1 complex with pimelate (c) 1:1 complex with suberate.

## Fluorescence Study

Sensitivity and selectivity of these receptors towards a series of dicarboxylates (malonate, succinate, glutarate, adipate, pimelate and suberate as their tetrabutylammonium salts) were evaluated by observing changes in their fluorescence emission spectra in DMSO. In the absence of dicarboxylates, **1** ($c = 4.03 \times 10^{-5}$ M) showed a characteristic emission band at 447 nm when excited at 355 nm. Upon addition of increasing amounts of guests, intensity of the emission band at 447 nm gradually decreased without producing any other spectral change (i.e., no spectral shift or formation of new emission band). Quenching of emission varied irregularly with the chain lengths of the dicarboxylates as revealed from the Stern–Volmer plot (Figure 6). The dicarboxylates of shorter chain lengths are more basic and hence induce stronger quenching although they are weakly complexed.

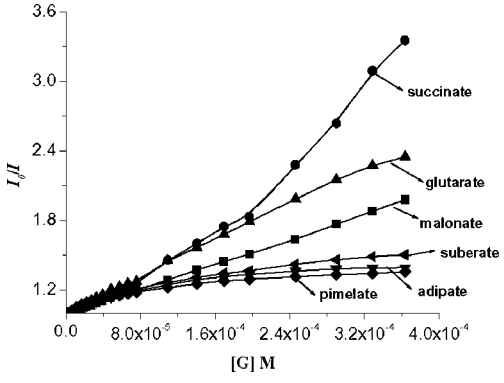


Figure 6. Stern–Volmer plot of **1** measured at 447 nm.

As a representative example, the corresponding change in emission spectra of **1** upon gradual addition of pimelate is displayed in Figure 7. From fluorescence study, it is evident that dicarboxylates of shorter chain lengths such as malonate, succinate and glutarate quench the emission of **1** significantly as compared to long-chain dicarboxylates although they do not exhibit remarkable changes in $^1$H NMR spectroscopy. This may be either due to the increase in ionic strength of the solution upon addition of large excess of dicarboxylates or due to different binding modes for which a change in dihedral angle around N-center of triphenylamine moiety occurs. This variation of the dihedral angle around N-center may have an effect on the excited state of the triphenylamine motif.

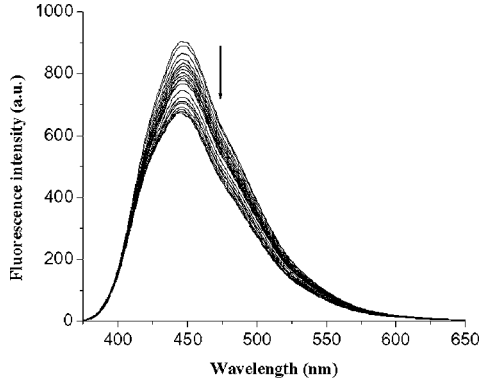


Figure 7. Change in fluorescence spectra of **1** ($c = 4.03 \times 10^{-5}$ M) in DMSO upon addition of pimelate.

The stoichiometries of the complexes of **1** were determined by Job's method,[15] where dicarboxylates of shorter chain length such as malonate, succinate and glutarate form 1:2 (host:guest) complexes and adipate, pimelate, suberate give rise to 1:1 (host:guest) complexes (Figure 8).

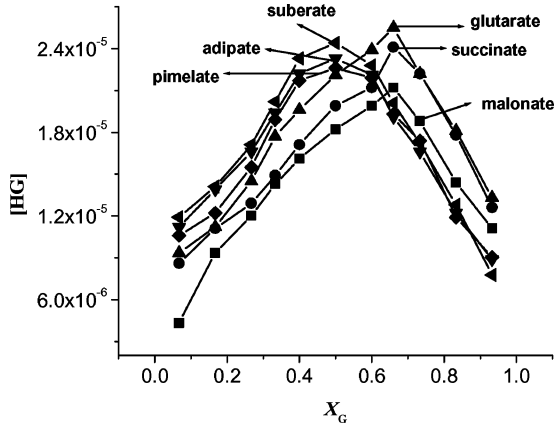


Figure 8. Fluoresence Job plot of **1** in presence of different guests. [H] + [G] = $4 \times 10^{-5}$ M.

In the similar process, the excited state properties of **2** were investigated in the presence of the same anions. In this case, receptor **2** ($c = 4.03 \times 10^{-5}$ M) in DMSO shows a sharp emission band at 443 nm when excited at 355 nm. On grad-

  

ual addition of the guest to the receptor solution of **2** the fluorescence intensity is decreased like with **1**. The Stern–Volmer plot (Figure 9) explains the quenching phenomena. Greater quenching is observed for long-chain dicarboxylates such as pimelate and suberate. This can be rationalised by better fitting of pimelate and suberate into the cavity of **2**. The nonlinear nature of the curves for **2** in Figure 9 (cf. Figure 6) suggests an interplay of both static and dynamic quenching. The change in emission of **2** upon increasing amounts of tetrabutylammonium pimelate is represented in Figure 10. Short-chain dicarboxylates such as malonate and succinate initially show smaller changes in fluorescence but in the presence of excess guest concentration, greater quenching of emission can be observed (Figure 9). The stoichiometry of the complexes was confirmed by fluorescence Job plots. A fluorescence Job plot of the receptor **2** (Figure 11) shows that host-guest complex concentration approaches a maximum when the mol fraction of guest is 0.5, which indicates 1:1 stoichiometry of the complex with the receptor. Glutarate, adipate, pimelate and suberate formed 1:1 complexes whereas short chain dicarboxylates such as malonate and succinate formed 1:2 (host/guest) complexes.

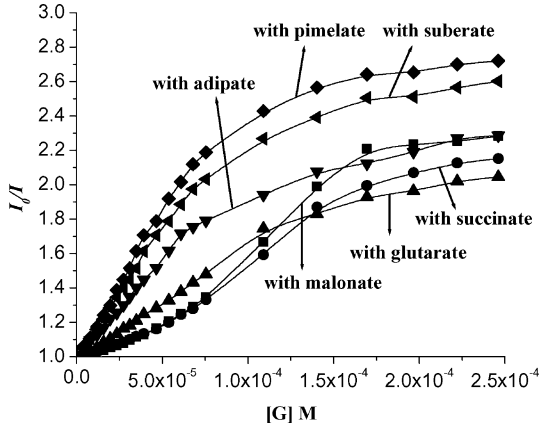


Figure 9. Fluorescence Stern–Volmer plot of **2** ($c = 4.03 \times 10^{-5}$ M) measured at 447 nm.

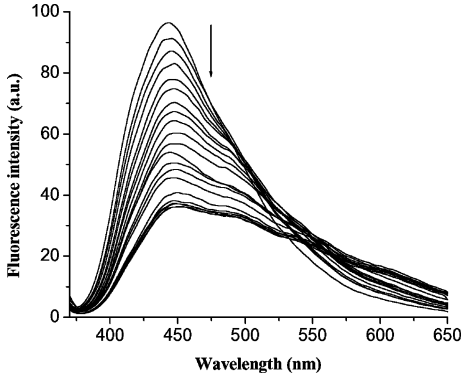


Figure 10. Change in fluorescence spectra of **2** ($c = 4.03 \times 10^{-5}$ M) in DMSO upon addition of pimelate.

In comparison, receptor **3** ($c = 5.2 \times 10^{-5}$ M) in DMSO shows a sharp emission band at 430 nm when excited at 355 nm. On addition of increasing amounts of the same

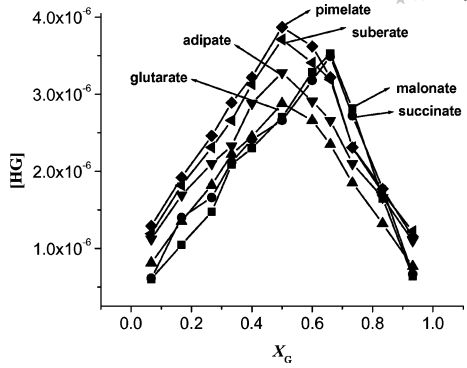


Figure 11. Fluoresence Job plot of **2** in presence of different guests. [H] + [G] = $4 \times 10^{-5}$ M.

guests, receptor **3** does not show any reliable and regular changes in fluorescence. Figure 12 shows the corresponding change in emission spectra of **3** in the presence of 9 equiv. amounts of different dicarboxylates. Such negligible perturbation of emission of **3** is indicative of the poor interaction with the anions. From these observations it is obvious that sufficient acidities of $H^o$ and $H^p$ protons of the pyridine nucleus are necessary for strong complexation.

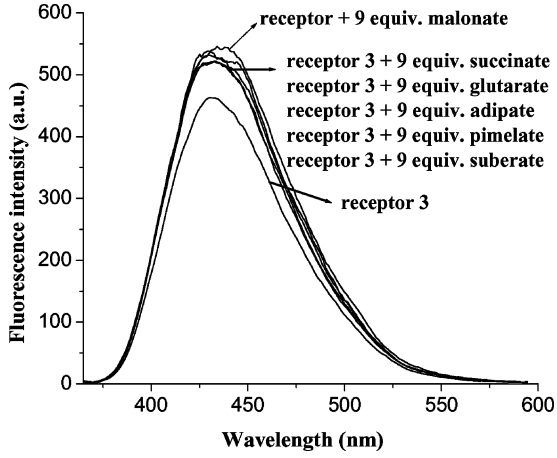


Figure 12. Change in fluorescence spectra of **3** ($c = 5.2 \times 10^{-5}$ M) in DMSO upon addition of 9 equiv. of different guests.

The quenching of emissions upon complexation is explained due to activation of a PET process active between the binding sites and excited state triphenylamine. The greater quenching of emission in **2** compared to **1** indicates that the PET process is more activated in **2** during complexation.

## UV/Vis Study

Recognition properties of the receptors **1**–**2** with various dicarboxylates in the ground state were simultaneously monitored by UV/Vis titrations in DMSO. In the absence of anion, receptor **1** ($c = 6.04 \times 10$–5 M) shows two absorption bands at 355 and 335 nm. With increase in guest concentration, intensities of the absorption peaks decreased to a minimum extent (Figure 13). This minor change in ab-

  

sorbance of **1** supports its typical PET behaviour. Compound **2** in DMSO ($c = 4.40 \times 10^{-5}$ M) shows characteristic absorption bands at 365, 335 and 295 nm. With increase in guest concentration, the intensities of absorption peaks at 365 and 335 nm increase gradually to different extents and vary with different guests (Figure 14). On progression of titration, the two peaks ultimately merge and became broad. Interestingly, in each case, an isosbestic point at 311 nm (not very sharp) is observed during titration. This can be explained with the formation of new species in solution. For example, Figure 15 shows the change in absorption of **2** in the presence of pimelate.

Receptor **3** exhibits negligible changes in absorbance in the presence of the same dicarboxylates as considered for receptors **1** and **2**. Thus **3** is a very weak host for dicarboxylates.

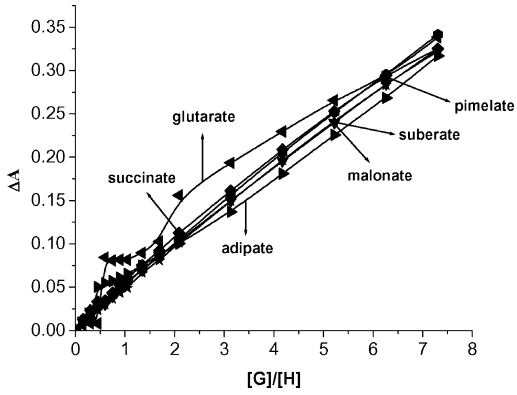


Figure 13. UV/Vis titration curves for **1** ($c = 6.04 \times 10$–$5$ M) measured at 355 nm.

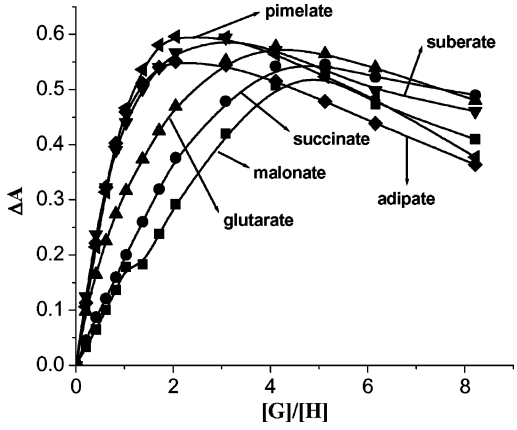


Figure 14. UV/Vis titration curves for **2** ($c = 4.4 \times 10^{-5}$ M) measured at 340 nm.

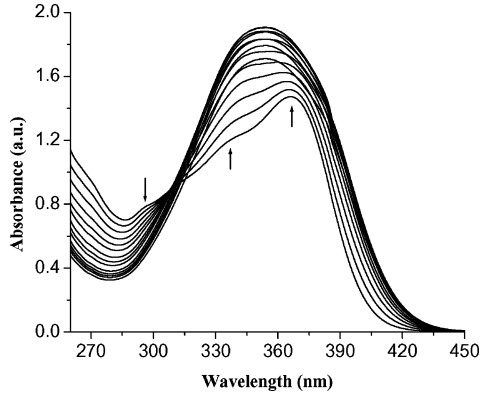


Figure 15. Change in UV/Vis spectra of **2** ($c = 4.4 \times 10^{-5}$ M) in DMSO upon addition of pimelate.

## Binding Constant Determination

The change of fluorescence intensity as a function of guest concentration leads to binding constant values for receptors **1** and **2** with the dicarboxylates according to Equations (1) and (2).

Equation (1) is valid for 1:1 host-to-guest complex stoichiometry.[16]

$$I = I_0 + (I_{lim} - I_0)/2C_H \{C_H + C_G + 1/K - [(C_H + C_G + 1/K)^2 - 4C_HC_G]^{1/2}\} \quad (1)$$

$I$ represents the intensity, $I_0$ represents the intensity of pure host, $C_H$ and $C_G$ are corresponding concentrations of host and anionic guests, respectively, $K$ is the binding constant. The binding constants $K$ and correlation coefficients $R$ were obtained from a non-linear least-square analysis of $I$ vs. $C_H$ and $C_G$.

Equation (2) describes 1:2 host-to-guest complex stoichiometry.[17]

$$I = (I_0 + I_1 \times K_1 \times C_G + I_{lim} \times K_1 \times K_2 \times C_G^2)/(1 + K_1 \times C_G + K_1 \times K_2 \times C_G^2) \quad (2)$$

$I$ represents the intensity, $I_0$ represents the intensity of pure host, $I_1$ is the intensity of 1:1 complex and $I_{lim}$ represents the intensity at infinite guest concentration. $K_1$ and $K_2$ are two binding constants for two successive steps.

As can be seen from Table 3, receptor **1** shows moderate binding toward aliphatic dicarboxylates with no measurable selectivity. In comparison, the open cleft of **2** exhibits higher binding constant values for long-chain dicarboxylates than **1** and represents a clear-cut selectivity for long-

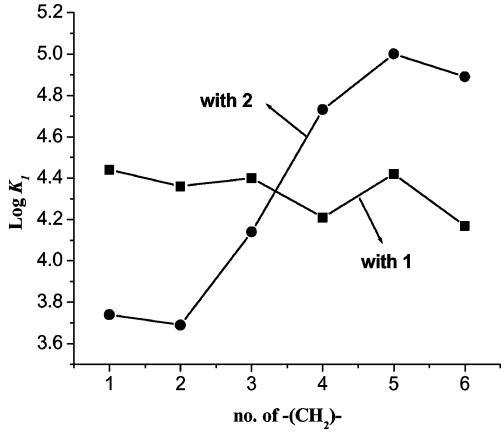


Figure 16. Comparison of binding constant values for receptors **1** and **2** with different aliphatic dicarboxylates in DMSO.

  

Table 3. Binding constants of receptor **1** and **2** with dicarboxylates in DMSO by fluorescence method.

| Guests (chain length in [Å])[a] | Receptor **1** $\log K_1$ | $\log K_2$ | $R^2$ | Receptor **2** $\log K_1$ | $\log K_2$ | $R^2$ |
|---|---|---|---|---|---|---|
| Malonate (2.26) | 4.44 ± 0.02 | 3.36 ± 0.03 | 0.9996 | 3.74 ± 0.02 | 4.31 ± 0.04 | 0.9961 |
| Succinate (3.97) | 4.36 ± 0.03 | 3.36 ± 0.05 | 0.9988 | 3.69 ± 0.03 | 4.37 ± 0.05 | 0.9955 |
| Glutarate (5.23) | 4.40 ± 0.04 | 3.63 ± 0.05 | 0.9985 | 4.14 ± 0.08 | | 0.9934 |
| Adipate (6.50) | 4.21 ± 0.02 | | 0.9990 | 4.73 ± 0.02 | | 0.9987 |
| Pimelate (7.77) | 4.42 ± 0.04 | | 0.9879 | 5.00 ± 0.01 | | 0.9996 |
| Suberate (9.04) | 4.17 ± 0.03 | | 0.9926 | 4.89 ± 0.01 | | 0.9997 |

[a] Distance between two carboxylate carbons, calculated for the gas phase.[14]

chain pimelate (see Figure 16). Increase in binding constants for **2** over the receptor **1** is attributed to the increase in acidity of $H^o$ and $H^p$ protons in **2**. Closer inspection of Table 3 reveals the different orders of $K_1$ and $K_2$ for **1** and **2**. Differential solvation, change in electron density at the binding centres, and mutual orientation of the binding arms of **1** and **2** are presumably the reasons for such differences in $K_1$ and $K_2$ for the complexes of 2:1 (guest/host) stoichiometries. Binding constant values for **3** were difficult to determine due to negligible change in its emission or absorption signal in the presence of dicarboxylates.

## Theoretical Investigation

A model study on the binding sites of the receptors **1**–**3** with the acetate ion was performed to identify their hydrogen bonding abilities. For this we considered the structures **1A**, **2A** and **3A** that were optimized individually and in the presence of acetate ion for gas-phase condition. Figure 17 displays the optimized geometries and the charge densities at different points of the model structures. The hydrogen bonding distances in the complexes of **1A**, **2A** and **3A** with acetate are also shown (Figure 17).

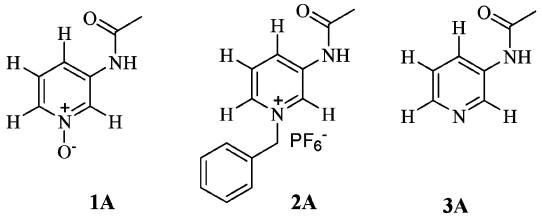


The dipole moments of receptors change on complexation, but the change is significant only for **2A** compared with the other structures **1A** and **3A** (Table 4). The shorter hydrogen bond lengths, and the much larger dipole moment change upon complexation for **2A** with acetate vis a vis **1A** and **3A** indicate greater affinity for the guest for this receptor. To test this idea further, we calculated the global electrophilicity index ($\omega$) of the three receptors; evidently the $\omega$ value is an order of magnitude larger for **2A** compared to **1A** and **3A**. The model thus establishes **2A** as a better complexation site for carboxylates, compared with the other two. This is reflected in the binding constant values as shown in Table 3.

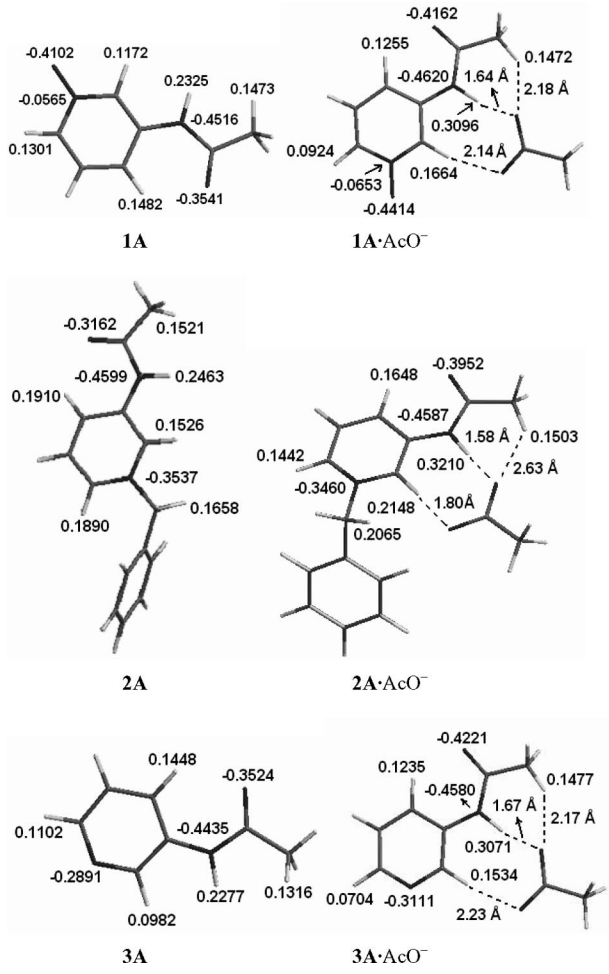


Figure 17. DFT-optimized structures of **1A**, **2A** and **3A** and their complexes with acetate ion showing charge densities at different atoms and hydrogen bonding characteristics.

Table 4. Dipole moment and global electrophilicity index of the model compounds and their complexes with acetate ion.

| Entry | Dipole moment (D) | $\omega$[a] |
|---|---|---|
| 1A | 3.234 | 0.2099 |
| 1A·AcO⁻ | 4.839 | |
| 2A | 3.045 | 1.1728 |
| 2A·AcO⁻ | 8.745 | |
| 3A | 2.553 | 0.1818 |
| 3A·AcO⁻ | 3.966 | |

[a] Global electrophilicity index.[18]

  

## Conclusions

We have described that pyridine *N*-oxide and pyridinium motifs in **1** and **2**, respectively, under the mastery of triphenylamine fluorescent probe are found to exhibit hydrogen bonding abilities for selective recognition of dicarboxylates. Between pyridine *N*-oxide and pyridinium motifs, pyridinium motif-based receptor **2** is efficient and effective for selective complexation of long-chain pimelate. The greater acidity of *ortho* and *para* protons and more electrophilic character of pyridinium binding sites of **2** as established from theoretical study are responsible factors for such effectiveness in the binding process. This is also reflected in large quenching of emission during complexation. Thus, receptor **2**, which is simple and easily accessible, can successfully be used as a sensor for size selective recognition of aliphatic dicarboxylate, especially pimelate in the present study.

## Experimental Section

**General Methods:** DMSO used for titration experiments was of 99.98+% HPLC grade. Chlorinated solvents were distilled from phosphorus pentoxide; THF was distilled from sodium, using benzophenone as indicator. Melting points are uncorrected. Flash column chromatography was carried out on silica gel 60–120 (Merck). Petroleum ether refers to the fraction with a boiling range of 40–60 °C.

**4-[4-Formyl(phenyl)anilino]benzaldehyde (4a):** To a solution of triphenylamine (8 g, 32.65 mmol) in dry DMF (65 mL), was added dropwise $POCl_3$ (31 mL, 332.65 mmol) at 0 °C from a dropping funnel fitted with a $CaCl_2$ guard tube. The reaction mixture was stirred at room temperature for 1 h and then mixture was warmed at 100 °C for 8 h. Reaction flask was cooled in an ice salt bath and the mixture was poured into ice, neutralized with NaOH solution, and then extracted with $CH_2Cl_2$ (4 × 200 mL). The organic layer was separated, dried with anhydrous $Na_2SO_4$ and removed under vacuum. The crude product was purified by column chromatography using 15% ethyl acetate in petroleum ether as eluent to give yellow solid **4a** (5.6 g, 57%); m.p. 140 °C (m.p. 142 °C[13]). FT-IR (KBr): $\tilde{\nu}$ = 3063, 2826, 2736, 1693, 1587, 1504, 1319, 1287, 1163 $cm^{-1}$.

**4-[4-Bromo(4-formylphenyl)anilino]benzaldehyde (5):** To a stirred solution of 4-[4-formyl(phenyl)anilino]benzaldehyde (**4a**) (1 g, 3.32 mmol) in dry $CHCl_3$ (50 mL), was added *N*-bromosuccinimide (0.65 g, 3.65 mmol). The reaction mixture was stirred under refluxing condition for 8 h. The precipitate formed was filtered off and washed with $CHCl_3$ and the filtrate was concentrated under vacuum. The organic portion was washed with 20% aqueous $NaHCO_3$ solution and extracted with $CHCl_3$ (3 × 40 mL). The organic layer was separated, dried with anhydrous $Na_2SO_4$ and removed on rotary evaporator. Crude product was purified by column chromatography using 15% ethyl acetate in petroleum ether to give **5** (1.07 g, 85%) as yellow solid; m.p. 158–160 °C. $^1$H NMR (500 MHz, $CDCl_3$, 25 °C): $\delta$ = 9.91 (s, 2 H), 7.77 (d, $J$ = 10 Hz, 4 H), 7.50 (d, $J$ = 10 Hz, 2 H), 7.18 (d, $J$ = 10 Hz, 4 H), 7.05 (d, $J$ = 10 Hz, 2 H) ppm. FT-IR (KBr): $\tilde{\nu}$ = 2801, 2726, 1694, 1588, 1574, 1488, 1273, 1166 $cm^{-1}$.

**4-[4-Bromo(4-carboxyphenyl)anilino]benzoic Acid (6):** To a stirred solution of **5** (1 g, 2.63 mmol) in 50 mL of acetone/water (4:1 *v*/*v*), $KMnO_4$ (2.1 g, 13.29 mmol) was added portion wise at 60 °C. The reaction mixture was stirred under refluxing condition for 8 h. The solvent was removed under vacuum and water (25 mL) was added. The black precipitate was filtered off and the filtrate was acidified with concd. aqueous HCl to give a white precipitate. The precipitate was filtered and washed with water for several times and dried under vacuum to give almost pure product **6** (0.87 g, 81%); m.p. 164–166 °C. $^1$H NMR (500 MHz, $CDCl_3$ + two drops of [$D_6$]DMSO, 25 °C): $\delta$ = 7.94 (d, $J$ = 10 Hz, 4 H), 7.43 (d, $J$ = 10 Hz, 2 H), 7.07 (d, $J$ = 10 Hz, 4 H), 7.01 ppm (d, $J$ = 10 Hz, 2 H), two protons for carboxylic acids were not found. FT-IR (KBr): $\tilde{\nu}$ = 3401, 2656, 2536, 1683, 1594, 1488, 1316, 1276 $cm^{-1}$.

**4,4′-[(4-Bromophenyl)imino]bis[*N*-(pyridin-3-yl)benzamide] (3):** Compound **6** (0.4 g, 0.97 mmol) was dissolved in dry $CH_2Cl_2$ (10 mL) and oxalyl chloride (1 mL, 13.44 mmol, excess) was added followed by addition of one drop of dry DMF. The reaction mixture was stirred at room temperature for 9 h under nitrogen atmosphere. The solvent was removed. The diacid chloride **7** was dried under vacuum (0.4 g, 92%) and an amount of this acid chloride (0.2 g, 0.45 mmol) was dissolved in dry THF (15 mL) and a mixture of 3-aminopyridine (0.085 g, 0.904 mmol) and triethylamine (0.3 mL, 2.17 mmol) in dry THF (5 mL) was added dropwise under nitrogen atmosphere. The reaction mixture was stirred at room temperature for 18 h. The solvent was evaporated and the residue was washed with 10% aqueous $NaHCO_3$ solution. The water layer was extracted with $CH_2Cl_2$ (3 × 25 mL). The organic layer was separated and dried with anhydrous $Na_2SO_4$ and removed under reduced pressure. The crude product was purified by column chromatography using 3% methanol in chloroform as eluent to give light yellow product **3** (0.17 g, 68%); m.p. 174–176 °C. $^1$H NMR (400 MHz, $CDCl_3$, 25 °C): $\delta$ = 8.65 (d, $J$ = 4 Hz, 2 H), 8.38 (d, $J$ = 4 Hz, 2 H), 8.29 (d, $J$ = 4 Hz, 2 H), 7.85 (s, 2 H), 7.80 (d, $J$ = 8 Hz, 4 H), 7.47 (d, $J$ = 8 Hz, 2 H), 7.34–7.30 (m, 2 H), 7.16 (d, $J$ = 8 Hz, 4 H), 7.03 (d, $J$ = 8 Hz, 2 H) ppm. $^{13}$C NMR (125 MHz, $CDCl_3$): $\delta$ = 166.3, 150.2, 145.4, 142.1, 135.8, 133.4, 129.4, 129.3, 128.8, 128.4, 127.8, 124.2, 123.2, 118.6 ppm. FTIR (KBr): $\tilde{\nu}$ = 3286, 1656, 1596, 1540, 1504, 1483, 1280 $cm^{-1}$. Mass ($ES^+$): 564.1 ($M^+$), 566.2 ($M^+$ + 2).

**Synthesis of 1:** To a solution of compound 3 (0.1 g, 0.177 mmol) in dry chloroform (15 mL) was added *m*-chloroperbenzoic acid (0.09 g, 0.54 mmol) and the reaction mixture was stirred under refluxing condition for 9 h under nitrogen atmosphere. The solvent was removed under reduced pressure and the crude product was directly used for purification. Purification was done by column chromatography using 8% methanol in chloroform as eluent to give white solid **1** (0.047 g, 45%); m.p. 306–308 °C. $^1$H NMR (400 MHz, [$D_6$]DMSO, 25 °C): $\delta$ = 10.53 (s, 2 H), 8.81 (s, 2 H), 7.99 (d, $J$ = 8 Hz, 2 H), 7.94 (d, $J$ = 8 Hz, 4 H), 7.67 (d, $J$ = 8 Hz, 2 H), 7.59 (d, $J$ = 8 Hz, 2 H), 7.39 (m, 2 H), 7.16 (d, $J$ = 8 Hz, 4 H), 7.10 (d, $J$ = 8 Hz, 2 H) ppm. $^{13}$C NMR (125 MHz, [$D_6$]DMSO, 25 °C): $\delta$ = 174.1, 150.4, 146.0, 139.4, 134.7, 133.7, 131.6, 130.5, 130.4, 129.1, 128.5, 126.9, 123.5, 117.6 ppm. FTIR (KBr): $\tilde{\nu}$ = 3251, 1673, 1594, 1575, 1504, 1488, 1270 $cm^{-1}$. Mass ($ES^+$): 596.0 ($M^+$), 598.1 ($M^+$ + 2). $C_{30}H_{22}BrN_5O_4$ (596.43): calcd. C 60.41, H 3.72, N 11.74; found C 60.38, H 3.77, N 11.79.

**Synthesis of 2:** To a solution of diamide **3** (0.03 g, 0.053 mmol) in dry $CH_3CN$ (5 mL) was added benzyl bromide (0.02 mL, 0.168 mmol) and the reaction mixture was stirred under refluxing condition for 22 h under nitrogen atmosphere. The solvent was concentrated in vacuo and petroleum ether was added to the reaction mixture followed by scratching of the wall of the flask. This process was done for several times and finally the precipitate was filtered to get solid product **8** (0.035 g, 73%). Compound **8** (0.03 g,

  

0.033 mmol) was dissolved in methanol (7 mL) and $NH_4PF_6$ (0.03 g, 0.184 mmol) was added to the solution. The reaction mixture was stirred at room temperature for 1 h. The solvent was concentrated and water (5 mL) was added to get a light green precipitate. The precipitate was filtered, washed with water for several times, dried in vacuo to give pure **2** (0.03 g, 88%); m.p. 148–150 °C. $^1$H NMR (400 MHz, [D$_6$]DMSO): $\delta$ = 11.11 (s, 2 H), 9.61 (s, 2 H), 8.96 (d, $J$ = 8 Hz, 2 H), 8.67 (d, $J$ = 8 Hz, 2 H), 8.17 (t, $J$ = 8 Hz, 2 H), 7.96 (d, $J$ = 8 Hz, 4 H), 7.62 (d, $J$ = 8 Hz, 2 H), 7.54 (d, $J$ = 8 Hz, 4 H), 7.47 (d, $J$ = 8 Hz, 6 H), 7.20 (d, $J$ = 8 Hz, 4 H), 7.11 (d, $J$ = 8 Hz, 2 H), 5.91 (s, 4 H) ppm. $^{13}$C NMR (125 MHz, [D$_6$]-DMSO): $\delta$ = 166.4, 150.7, 140.6, 140.2, 136.2, 136.1, 134.9, 133.9, 130.8, 130.4, 130.2, 129.7, 129.2, 128.9, 127.9, 123.4, 123.0, 118.5, 64.7 ppm. FTIR: $\tilde{\nu}$ = (KBr): 3399, 3107, 1681, 1591, 1505, 1439, 1256 cm$^{-1}$. Mass (ES$^+$): 890.0 ($M^+ - PF_6$), 654.0 ($M^+ - 2PF_6 - 1$), 576.3.

**General Procedure for Fluorescence Titration:** Stock solutions of the receptors were prepared in UV grade DMSO and 2.5 mL of each receptor solution was taken in the cuvette. The solution was irradiated at the selected excitation wavelength. Upon addition of a guest compound (dissolved in DMSO), the change in fluorescence emission of the receptor was observed. The corresponding emission values during titration were recorded and used for the determination of binding constant values. The change in emission in the presence of different amounts of guest dicarboxylates was used to have the Stern–Volmer plot.

**General Procedure for UV/Vis Titration:** Stock solutions of the receptors were prepared in UV grade DMSO and 2.5 mL of each receptor solution was taken in the cuvette. Dicarboxylate guest (dissolved in DMSO) was added in different amounts to the receptor solution. The corresponding absorbance values during titration were noted.

**Computational Study:** Structures **1A**, **2A** and **3A** were optimised for gas phase conditions at DFT (6-311G**[19] and B3LYP[20]) level, individually and in presence of acetate ion. Figures of MO levels (HOMO, HOMO-1, LUMO and LUMO+1) are given in Supporting Information The Gaussian-03 package[21] and GAMESS-US suite[22] (version April 11, 2008) were used for the calculations and the MO figures were obtained using the MaSK software.[23]

**Supporting Information** (see also the footnote on the first page of this article): Fluorescence and absorption spectra of **1** and **2** in the presence of different guests, binding constants determination for **1** and **2** with the dicarboxylates, $^1$H and $^{13}$C NMR spectra of **1**–**3**, MO pictures of the model structures **1A**, **2A** and their complexes with acetate ion, energy-optimized structures of **2** with different dicarboxylates.

## Acknowledgments

We thank Council of Scientific and Industrial Research (CSIR), New Delhi, India for financial support.

[1] a) R. Martinez-Manez, F. Sancenon, *Chem. Rev.* **2003**, *13*, 4419–4476; b) C. Suksai, T. Tuntulani, *Chem. Soc. Rev.* **2003**, *32*, 192–202; c) P. D. Beer, P. A. Gale, *Angew. Chem. Int. Ed.* **2001**, *40*, 486–516; d) F. P. Schmidtchen, M. Berger, *Chem. Rev.* **1997**, *97*, 1609–1646.

[2] a) D. Voet, J. G. Voet, *Biochemistry*, 2nd ed., John Wiley & Sons, New York, NY, **1995**; b) T. Gunnlaugsson, A. P. Davis, J. E. ÓBrien, M. Glynn, *Org. Lett.* **2002**, *4*, 2449–2452 and references cited therein.

[3] P. Cudic, J. P. Vigneron, J. M. Lehn, M. Cesario, T. Prange, *Eur. J. Org. Chem.* **1999**, 2479–2484.

[4] a) A. Echavarren, A. Galan, J. de Mendoza, *J. Am. Chem. Soc.* **1989**, *111*, 4994–4995; b) J. Raker, T. E. Glass, *J. Org. Chem.* **2002**, *67*, 6113–6116.

[5] a) M. Boiocchi, M. Bonizzoni, L. Fabbrizzi, G. Piovani, A. Taglietti, *Angew. Chem. Int. Ed.* **2004**, *43*, 3847–3852; b) M. Bonizzoni, L. Fabbrizzi, G. Piovani, A. Taglietti, *Tetrahedron* **2004**, *60*, 11159–11162.

[6] S. K. Kim, B.-G. Kang, H. S. Koh, Y. J. Yoon, S. J. Jung, B. Jeong, K.-D. Lee, J. Yoon, *Org. Lett.* **2004**, *6*, 4655–4658 and references cited therein.

[7] a) S.-Y. Liu, L. Fang, Y.-B. He, W.-H. Chan, K.-T. Yeung, Y.-K. Cheng, R.-H. Yang, *Org. Lett.* **2005**, *7*, 5825–5828; b) S.-Y. Liu, Y.-B. He, W. H. Chan, A. W. M. Lee, *Tetrahedron* **2006**, *62*, 11687–11696; c) S.-Y. Lin, Y.-B. He, J.-L. Wu, L.-H. Wei, H.-J. Qin, L.-Z. Meng, L. Hu, *Org. Biomol. Chem.* **2004**, *2*, 1582–1586; d) V. D. Jadhav, F. P. Scmidtchen, *Org. Lett.* **2006**, *8*, 2329–2332 and references cited therein.

[8] a) D. R. Turner, M. J. Paterson, J. W. Steed, *J. Org. Chem.* **2006**, *71*, 1598–1608; b) J. M. Russell, A. D. M. Parker, I. Radosavljevic-E, J. A. K. Howard, J. W. Steed, *Chem. Commun.* **2006**, 269–271.

[9] S. Metzger, B. Lippert, *J. Am. Chem. Soc.* **1996**, *118*, 12467–12468.

[10] P. Auffinger, S. Louise-May, E. Westhof, *J. Am. Chem. Soc.* **1996**, *118*, 1181–1189.

[11] a) G. R. Desiraju, *Acc. Chem. Res.* **1991**, *24*, 290–296; b) T. Steiner, W. Saenger, *J. Am. Chem. Soc.* **1992**, *114*, 10146–10154; c) C. V. K. Sharma, G. R. Desiraju, *J. Chem. Soc. Perkin Trans. 2* **1994**, 2345–2352; d) T. Steiner, *J. Chem. Soc. Perkin Trans. 2* **1995**, 1315–1319; e) J. D. Chaney, C. R. Goss, K. Folting, B. D. Santarsiero, M. D. Hollingworth, *J. Am. Chem. Soc.* **1996**, *118*, 9432–9433; f) O. B. Berryman, D. W. Johnson, *Chem. Commun.* **2009**, 3143–3153 and references cited therein; g) R. Custelcean, D. Jiang, B. P. Hay, W. Luo, B. Gu, *Cryst. Growth Des.* **2008**, *8*, 1909–1915; h) P. A. Gal, M. B. Hursthouse, M. E. Light, J. L. Sessler, C. N. Warriner, R. S. Zimmerman, *Tetrahedron Lett.* **2001**, *42*, 6759–6762; i) J. W. Steed, *Chem. Commun.* **2006**, 2637–2649.

[12] K. Ghosh, G. Masanta, *Tetrahedron Lett.* **2006**, *47*, 2365–2369.

[13] a) G. Lai, X. R. Bu, J. Santos, E. A. Mintz, *Synlett* **1997**, 1275–1276; b) T. Mallegol, S. Gmouh, M. A. A. Meziane, M. Blanchard-Desce, O. Mongin, *Synthesis* **2005**, 1771–1774.

[14] Energy minimization was carried out by *MMX* (PC Model) Serena Software, **1993**. Molecular modeling was performed by using standard constants, and the dielectric constant was maintained at 1.5.

[15] P. Job, *Ann. Chim.* **1928**, *9*, 113–203.

[16] a) B. Valeur, J. Pouget, J. Bourson, M. Kaschke, N. P. Eensting, *J. Phys. Chem.* **1992**, *96*, 6545–6549; b) J. Bourson, J. Pouget, B. Valeur, *J. Phys. Chem.* **1993**, *97*, 4552–4557.

[17] a) S. Fukuzumi, Y. Kondo, S. Mochizuki, T. Tanaka, *J. Chem. Soc. Perkin Trans. 2* **1989**, 1753–1761; b) A. Tsuda, C. Fkumoto, T. Oshima, *J. Am. Chem. Soc.* **2003**, *125*, 5811–5822.

[18] P. K. Chattaraj, U. Sarkar, D. R. Roy, *Chem. Rev.* **2006**, *106*, 2065–2091.

[19] R. Krishnan, J. S. Binkeley, R. Seeger, J. A. Pople, *J. Chem. Phys.* **1980**, *72*, 650–654.

[20] a) A. D. Becke, *J. Chem. Phys.* **1993**, *98*, 5648–5652; b) P. J. Stephens, F. J. Devlin, C. F. Chabalowski, M. J. Frisch, *J. Phys. Chem.* **1994**, *98*, 11623–11627.

[21] *Gaussian 03*, Revision C.01, M. J. Frisch, G. W. Trucks, H. B. Schlegel, G. E. Scuseria, M. A. Robb, J. R. Cheeseman, J. A. Montgomery Jr., T. Vreven, K. N. Kudin, J. C. Burant,J. M. Millam, S. S. Iyengar, J. Tomasi, V. Barone, B. Mennucci, M. Cossi, G. Scalmani, N. Rega, G. A. Petersson, H. Nakatsuji, M. Hada, M. Ehara, K. Toyota, R. Fukuda, J. Hasegawa, M. Ishida, T. Nakajima, Y. Honda, O. Kitao, H. nakai, M. Klene, X. Li, J. E. Knox, H. P. Hratchian, J. B. Cross, C. Adamo, J.

  

Jaramillo, R. Gomperts, R. E. Stratmann, O. Yazyev, A. J. Austin, R. Cammi, C. Pomelli, J. W. Ochterski, P. Y. Ayala, K. Morokuma, G. A. Voth, P. Salvador, J. J. Dannenberg, V. G. Zakrzewski, S. Dapprich, A. D. Daniels, M. C. Strain, O. Farkas, D. K. Malick, A. D. Rabuck, K. Raghavachari, J. B. Foresman, J. V. Ortiz, Q. Cui, A. G. Baboul, S. Clifford, J. Cioslowski, B. B. Stefanov, G. Liu, A. Liashenko, P. Piskorz, I. Komaromi, R. L. Martin, D. J. Fox, T. Keith, M. A. Al-Laham, C. Y. Peng, A. Nanayakkara, M. Challacombe, P. M. W. Gill, B. Johnson, W. Chen, M. W. Wong, C. Gonzalez and J. A. Pople, Gaussian, Inc., Wallingford CT, **2004**.

[22] a) M. W. Schmidt, K. K. Baldridge, J. A. Boatz, S. T. Elbert, M. S. Gordon, J. H. Jensen, S. Koseki, N. Matsunaga, K. A. Nguyen, S. Su, T. L. Windus, M. Dupuis, J. A. Montgomery, *J. Comput. Chem.* **1993**, *14*, 1347; b) M. S. Gordon, M. W. Schmidt, in: *Theory and Applications of Computational Chemistry: The first forty years* (Eds.: C. E. Dykstra, G. Frenking, K. S. Kim, G. E. Scuseria), p. 1167, Elsevier, Amsterdam, **2005**.

[23] Y. Podolyan, J. Leszczynski, *Int. J. Quantum Chem.* **2009**, *109*, 8–16.

Received: May 1, 2009
Published Online: July 27, 2009

  